ELSEVIER

Thermochimica Acta 374 (2001) 115–128

thermochimica acta

www.elsevier.com/locate/tca

A study of the thermal decomposition of copper(II) and zinc(II) malonate, maleate and succinate complexes using direct current electrical conductivity measurements

A.K. Nikumbh*, S.K. Pardeshi, M.N. Raste

Department of Chemistry, University of Pune, Ganeshkhind, Pune 411007, India

Received 19 July 2000; received in revised form 5 February 2001; accepted 5 February 2001

Abstract

The comparative study of the thermal analysis (thermogravimetric analysis (TGA), differential scanning calorimetry (DSC) and derivative thermogravimetry (DTG)) and dc electrical conductivity measurements of copper(II) and zinc(II) malonate, maleate and succinate complexes have been carried out using the atmospheres of static air and dynamic dry nitrogen. The isothermally heated products at each decomposition stage have been characterized by C and H analyses, infrared spectra and X-ray powder diffraction data. The electrical conductivity measurements were found to give additional information on the solid-state reaction as compared to that obtained from conventional thermal techniques (such as TGA, DTG and DSC).

Keywords: Thermal decomposition; Dicarboxylates; Electrical conductivity; Solid-state reaction; Decomposition processes

1. Introduction

Thermal investigations concerned with the characterization of the mechanisms of solid-state decompositions have included many studies of the thermal reactions of oxalates, some of which have been the subject of multiple independent examinations by different groups of workers [1–3]. Boldyrev et al. [4] have classified these reactions on the basis of the principal residual product (carbonate, oxide or metal) which depends on the electropositivity of the cation. These workers identify the initial step in all oxalate decompositions as the rupture of the C–C bond in the anion. The literature on this group of decompositions is extensive and several salts, notably nickel oxalate and silver oxalate, have been examined in particular detail [3]. It has been shown [5] that the decomposition of copper(II) malonate proceeds to completion through two distinct rate processes. The second of these reactions was the decomposition of copper(I) malonate, and the reaction also involved melt formation together with acetate formation. Similarly copper(II) fumarate and copper(II) maleate [6–8], copper(II) succinates [9–14], copper(II) malonate [15–20] and copper(II) tartarate [21] decomposed with the intervention of copper(I) salts. Thus the decomposition of these copper(II) carboxylates proceed with stepwise cation reduction, $Cu^{2+} \rightarrow Cu^{+} \rightarrow Cu^{0}$, a common chemical characteristic within a field where behavioral similarities between related reactants are unusual [3].

* Corresponding author. Tel.: +91-20-5656061,5651728; fax: +91-20-5651728.
E-mail address: aknik@chem.unipune.ernet.in (A.K. Nikumbh).

0040-6031/01/$ – see front matter
PII: S0040-6031(01)00483-X

The thermal decomposition of the dicarboxylates of bivalent transition metals (Mn, Fe, Co, Ni, Cu and Zn) have been investigated by mainly thermal analysis, evolved gas analysis and BET surface area measurements in the atmospheres of N_2, CO_2, and O_2 in the air [7,11,18,21–24]. It has also been shown that CO_2 has an inhibiting effect on the decomposition whereas O_2 and air have the accelerating effects on the basis of N_2.

In above literature, thermogravimetric analysis (TGA), differential thermal analysis (DTA) and derivative thermogravimetry (DTG), supplemented with X-ray diffraction data, have been used to study the progress of thermal decomposition of copper(II) and zinc(II) dicarboxylates. In such a study it was not possible to characterize the temperature at which different oxides from these dicarboxylates could be obtained in air, since a broad exothermic peak was obtained. It would therefore be profitable to use another technique which may help to differentiate these various steps of the solid-state reaction. The present work is concerned with the feasibility of using direct current electrical conductivity measurements as a probe to study the progress of the thermal decomposition of copper(II) and zinc(II) malonate, maleate and succinate complexes. The conductivity measurements were supplemented with data obtained by TGA, DTG, DSC, X-ray diffraction and infrared spectroscopy.

2. Experimental

Copper(II) and zinc(II) malonate, maleate and succinate complexes were synthesized according to usual procedures as described in [24,25].

The procedure used for measurement of direct current electrical conductivity, infrared spectroscopy and X-ray powder diffraction were similar to those reported earlier [26,27].

3. Results and discussion

3.1. Characterization of copper(II) and zinc(II) dicarboxylates

The elemental analyses made in wt.% of copper(II) and zinc(II) dicarboxylates (i.e. malonate, maleate and succinate) are very well matched with calculated ones (Table 1). The presence of water of crystallization for these complexes was confirmed on the basis of the thermal analysis curves. These results are further supplemented by infrared spectroscopic measurements. The bidentate linkage of dicarboxylate group with metal was confirmed on the basis of the difference between the antisymmetric and symmetric stretching frequencies [28]. The copper(II) malonate, maleate and succinate and zinc(II) malonate complexes exhibit a chain-like polymeric octahedral structure (i.e. carboxylates di-anion bonded to two different metal atoms), while zinc(II) maleate and succinate complexes exhibit a layer-type polymeric octahedral structure (i.e. two molecules of the carboxylate anion bonded to each metal ion), which have been assigned by infrared spectra [24]. The room temperature magnetic moments (Table 1) are in good agreement with the spin only values of Cu^{2+} for copper(II) dicarboxylates and zero spin of Zn^{2+} for zinc(II) dicarboxylates, which indicates that the compounds have free spin with sp^3d^2 hybridization [29].

3.2. Thermal decomposition processes of copper(II) and zinc(II) malonate, maleate and succinate complexes

3.2.1. Static air atmosphere

3.2.1.1. Copper(II) dicarboxylates. In Fig. 1(a) to (c), for copper(II) malonate monohydrate ($CuC_3H_2O_4 \cdot H_2O$), copper(II) maleate monohydrate ($CuC_4H_2O_4 \cdot H_2O$) and copper(II) succinate half hydrate ($CuC_4H_4O_4 \cdot 0.5H_2O$), the DSC and DTG curves showed a peak at around 150°C for dehydration step under static air atmosphere. TGA curves also produced a mass loss beginning at 60 to 210°C corresponded to the removal of water molecules from these complexes. The broad exothermic peak corresponding to oxidative decomposition were shown on DSC curves at around 290°C and a peak at these temperatures were also seen on DTG curves. The TGA curves showed a continuous mass loss in this region, where the material finally crystallized to CuO in this atmosphere. Above 340°C the lifting up mass loss were observed on TGA curves for these complexes. This may be due to the non-stoichiometry (or defects) present in the final product. The observed mass losses and the corresponding temperature ranges are given in Table 2.

Table 1
Analytical data of copper(II) and zinc(II) dicarboxylates

Compound	Formula	Formula weight	Elemental analysis (wt.%)						Magnetic moment (μ) B.M.
			C		H		Metal		
			Calculated	Found	Calculated	Found	Calculated	Found	
Copper(II) malonate monohydrate	$CuC_3H_2O_4{\cdot}H_2O$	183.54	19.61	18.93	2.18	2.57	34.62	33.79	1.98
Copper(II) maleate monohydrate	$CuC_4H_2O_4{\cdot}H_2O$	195.54	24.54	25.12	2.04	1.99	32.49	32.11	1.74
Copper(II) succinate half hydrate	$CuC_4H_4O_4{\cdot}0.5H_2O$	188.54	25.40	24.98	2.65	2.68	33.70	33.77	1.84
Zinc(II) malonate dihydrate	$ZnC_3H_2O_4{\cdot}2H_2O$	203.37	17.70	17.68	2.95	2.93	32.14	31.74	Diamagnetic
Zinc(II) maleate dihydrate	$Zn(C_4H_3O_4)_2{\cdot}2H_2O$	331.37	28.97	28.90	1.81	1.79	19.72	19.89	Diamagnetic
Zinc(II) succinate one and half hydrate	$Zn(C_4H_5O_4)_2{\cdot}1.5H_2O$	326.37	29.41	29.38	3.98	3.92	20.03	20.21	Diamagnetic

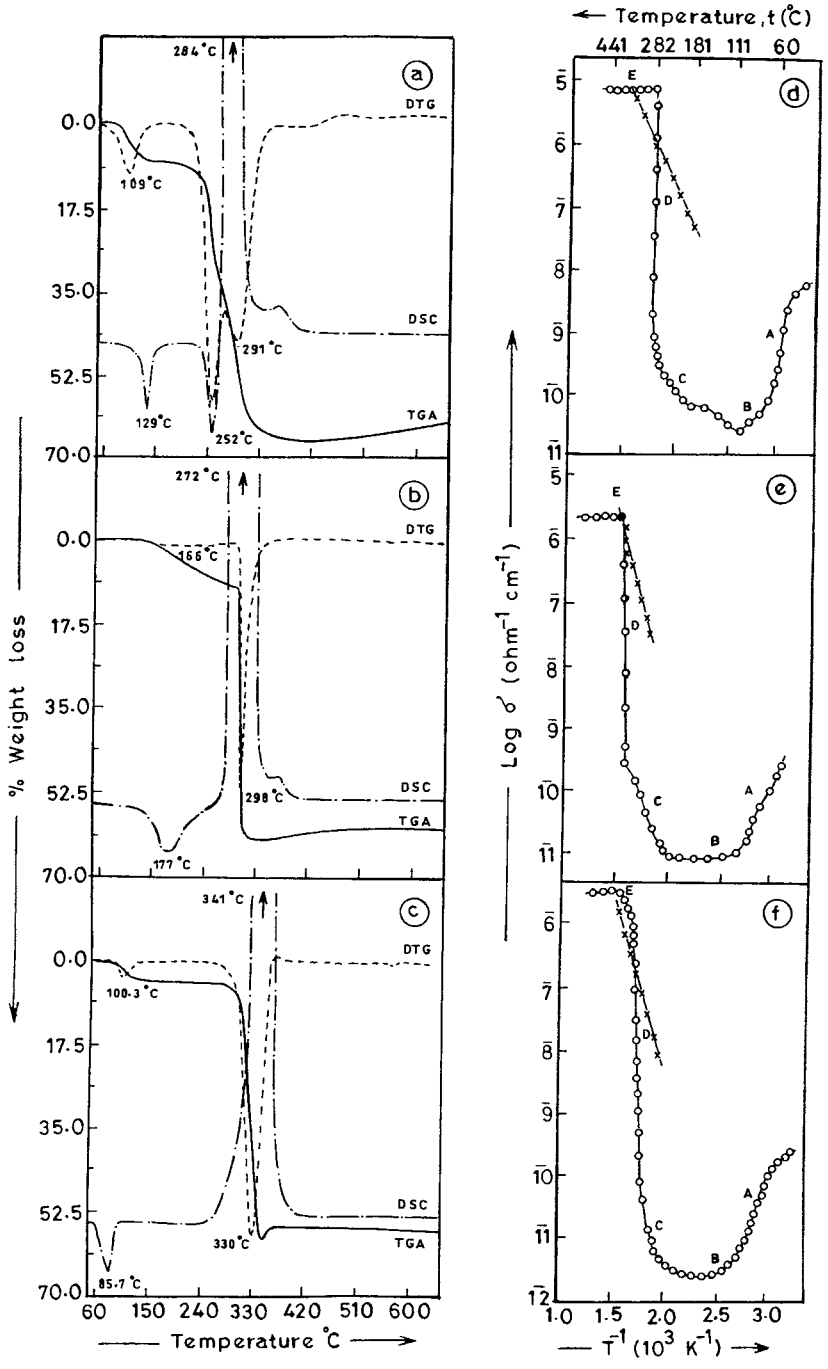

Fig. 1. Thermal decomposition of copper(II) dicarboxylates in a static air atmosphere. TGA, DTG and DSC curves for (a) $CuC_3H_2O_4{\cdot}H_2O$; (b) $CuC_4H_2O_4{\cdot}H_2O$; (c) $CuC_4H_4O_4{\cdot}0.5H_2O$. Plot of log σ vs. T^{-1} for (d) $CuC_3H_2O_4{\cdot}H_2O$; (e) $CuC_4H_2O_4{\cdot}H_2O$; (f) $CuC_4H_4O_4{\cdot}0.5H_2O$; ($\odot$) during decomposition; ($\times$) cooling cycle.

Table 2
TGA–DTG–DSC data of copper(II) dicarboxylates under static air atmosphere

Compound	TGA			DTG peak temperature (°C)	DSC peak temperature (°C)
	Mass loss (%)		Temperature range (°C)		
	Observed	Calculated			
Copper(II) malonate monohydrate	9.23	9.80	35–170	108.9	129.9 (endo.)
$CuC_3H_2O_4{\cdot}H_2O$	36.45	37.85	170–275	251.7	245.4 (endo.)
	21.87	22.68	275–380	290.8	284.4 (exo.)
Copper(II) maleate monohydrate	9.72	9.20	35–210	165.3	177.0 (endo.)
$CuC_4H_2O_4{\cdot}H_2O$	53.47	55.19	210–375	298.7	271.7 (exo.)
Copper(II) succinate half hydrate	4.37	4.77	35–180	100.3	85.7 (endo.)
$CuC_4H_4O_4{\cdot}0.5H_2O$	54.44	55.69	180–385	330.0	341.4 (exo.)

The thermal stabilities of metal dicarboxylates can be found; in general, the temperature of initial weight loss values from TGA provide more accurate information than maximum temperature of DTG. However, when the temperature of initial weight loss values are somewhat difficult to measure with sufficient accuracy, the maximum temperature of DTG values should be preferred, provided the latter are sharp [30]. Comparison of the temperature of initial weight loss values for dehydration (see Table 2) leads to the stability sequence: $CuC_4H_2O_4{\cdot}H_2O > CuC_4H_4O_4{\cdot}0.5H_2O > CuC_3H_2O_4{\cdot}H_2O$. The order of stabilities may be explained either on the basis of the tendency of the central metal ions to capture the electron from the respective ligand [31] or on the size of the chelate ring formed by the ligand to the central metal ion. The temperature of decomposition of these anhydrous complexes are fairly close to each other (Table 2).

The temperature variation of electrical conductivity σ (Fig. 1(d) to (f)) did show a steady decrease in σ between room temperature to 85°C (Region A) and the value then remained nearly constant up to 175°C (Region B). There was a steady increase in σ between 180 to 270°C (Region C), followed by a steep increase at 280°C to a maximum at 400°C (Region D). The σ value then remained almost constant in the temperature range 400–450°C (Region E).

A comparison of thermal analysis (TGA, DTG and DSC) with conductivity analysis in this atmosphere of $CuC_3H_2O_4{\cdot}H_2O$, $CuC_4H_2O_4{\cdot}H_2O$ and $CuC_4H_4O_4{\cdot}0.5H_2O$ shows that the conductivity analysis gives a much more detailed view of the decomposition process. TGA showed a continuous weight loss, and the DSC curves showed only one broad exothermic peak, the various metastable intermediates formed during this oxidative decomposition step could not be determined in detail. However, the direct current electrical conductivity, represented in Fig. 1(d) to (f), gave complete information on the intermediates by showing different regions of conductivity.

The analysis of the plot of $\log \sigma$ versus T^{-1} must include due consideration of the physical factors involved in the transformation of a compound (formed during a chemical reaction) in the amorphous phase of the fusion layers to large crystallites, though the probable intermediate stages, such as the formation of a fine network of grain boundaries and subsequent consolidation, and the formation of defects and subsequent annealing of such defects. It is therefore necessary to supplement the electrical conductivity measurements with other measurements of the structural characteristics of the samples, such as measurements of infrared spectra and X-ray diffraction patterns.

The plot of $\log \sigma$ versus T^{-1} in Fig. 1(d) to (f) showed a Region B at 85–210°C for dehydration step of $CuC_3H_2O_4{\cdot}H_2O$, $CuC_4H_2O_4{\cdot}H_2O$ and $CuC_4H_4O_4{\cdot}0.5H_2O$. The isothermally heated copper(II) malonate, copper(II) maleate and copper(II) succinate samples under static air, at 140, 200 and 150°C, respectively, showed the absence of the –OH band and a considerable reduction in the intensities of all the bands. The X-ray diffraction pattern showed polycrystallinity of the samples with decrease in interplanar spacings as

compared to the parent compounds. The elemental analyses were in good agreement with the respective anhydrous samples. Region B of the plot of $\log \sigma$ versus T^{-1} shown in Fig. 1(d) to (f) could be therefore related to dehydration of the dicarboxylates. Such a change is probably associated with a change from an octahedral geometry of copper(II) to tetrahedral form.

After dehydration step the value of σ increase steadily from 210 to 280°C (Region C). The infrared spectra of the isothermally heated parent samples at these regions showed a decrease in the intensities of coordinated carboxylate bands and the appearance of new and strong bands in the oxide region occurred at 514 and 484 cm^{-1} due to presence of cuprous oxide [32]. The X-ray diffraction pattern of these isothermally heated samples were generally broad. The pattern fitted well with the anhydrous copper(II) dicarboxylates and Cu_2O. A sharp increase in the value of σ was observed within the temperature range 280–310°C (Region D). For the samples heated isothermally at 300°C, the infrared spectra showed a weak band corresponding to carboxylate group, but a strong band was observed at 484 cm^{-1}. The X-ray diffraction pattern of these isothermally heated samples in this region were complex, probably corresponding to the mixture of anhydrous copper(II) dicarboxylates, Cu_2O and CuO. Thus the steep increase in the conductivity observed in Region D was due to the transformation of anhydrous copper(II) dicarboxylates to CuO, possibly via the semiconducting Cu_2O ($\sim 10^{-6}\,\Omega^{-1}\,cm^{-1}$) [33]. Within the temperature range of Region E in Fig. 1(d) to (f), the value of σ remained almost constant. The samples obtained by heating isothermally in static air at 360°C showed a black oxide. The X-ray diffraction pattern observed for samples in this region indicated a predominance of CuO. No line which could be assigned to metallic copper was detected in our work. The sample thus obtained at 360°C shows a change in σ as the temperature is changed.

3.2.1.2. Zinc(II) dicarboxylates. TGA, DTG and DSC curves of zinc(II) malonate dihydrate ($ZnC_3H_2O_4 \cdot 2H_2O$), zinc(II) maleate dihydrate ($Zn(C_4H_3O_4)_2 \cdot 2H_2O$) and zinc(II) succinate one and half hydrate ($Zn(C_4H_5O_4)_2 \cdot 1.5H_2O$) in static air are shown in Fig. 2(a) to (c). The dehydration took place in a single step for these dicarboxylates. The observed mass losses are reasonable with calculated values (Table 3). The decomposition of zinc(II) maleate and zinc(II) succinate were indicated by endothermic peak at 160 and 231°C followed by a strong exothermic peak at 421 and 485°C, respectively, on DSC curves, while a broad exothermic peak with hump at 388°C was obtained for zinc(II) malonate complex. The peaks at this temperature were also seen on DTG curves. The TGA curves showed two-step decomposition processes in the temperature range 150–260 and 260–480°C. The mass losses in this region were found to be in good agreement with the formation of ZnO (Table 3). The complete data for the observed mass losses and the corresponding temperature ranges are given in Table 3. It is interesting to observe here that, the zinc(II) malonate, maleate and succinate are thermally much stabler than the corresponding copper(II) salts. This is in accordance with the strengths of the M–O bonds, the Zn–O bond being stronger than the Cu–O bond, as seen from the square of the differences in the electronegativities [34].

Region B in the plots of $\log \sigma$ versus T^{-1} (Fig. 2(d) to (f)) corresponds to the dehydration of zinc(II) malonate, zinc(II) maleate and zinc(II) succinate complexes. The elemental analyses, infrared spectra and X-ray diffraction pattern, for isothermally heated samples in this region confirms the formation of anhydrous zinc(II) dicarboxylates. After dehydration step, the value of σ remains constant upto 250°C for zinc(II) malonate, while the value of σ increase steadily from 140 to 210°C and then decreases upto 250°C (Region B′) for zinc(II) maleate and zinc(II) succinate. The sample obtained on isothermal heating of zinc(II) malonate at 200°C showed the infrared spectra and X-ray diffraction pattern are similar to anhydrous compound. The infrared spectra of the isothermally heated zinc(II) maleate and zinc(II) succinate at 230°C exhibited a carboxylate group frequencies; no band was found at 1685 cm^{-1} indicating the absence of carboxyl (–COOH) group. The infrared spectra do not show the presence of zinc carbonate or ZnO bond formation. No X-ray diffraction lines due either to zinc carbonate or zinc oxide were observed; thus the possibility of the formation of zinc carbonate or zinc oxide can easily be ruled out. The X-ray diffraction pattern of these isothermally heated samples showed the structure to be polycrystalline in nature; the peak corresponding to $ZnC_4H_2O_4$ or $ZnC_4H_4O_4$ were

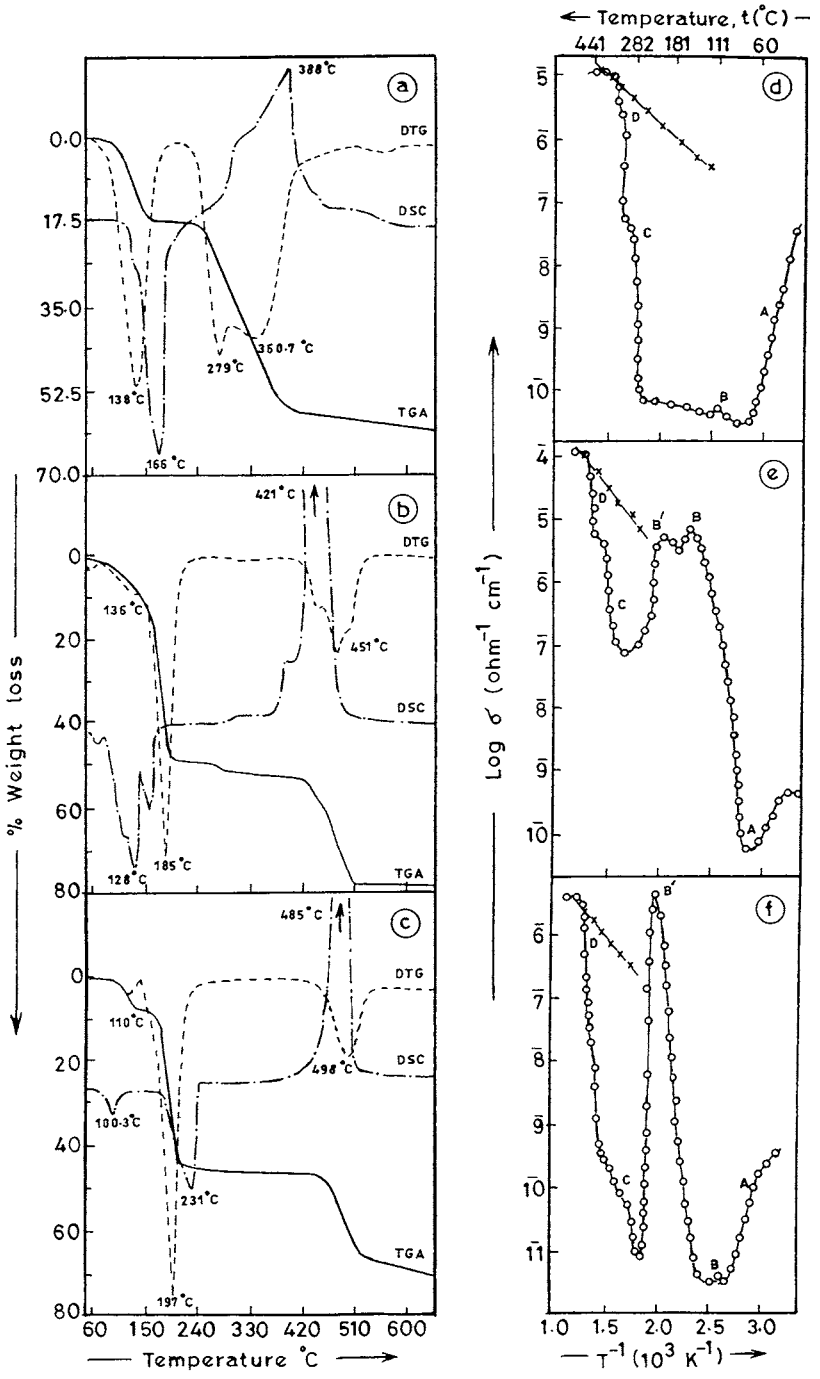

Fig. 2. Thermal decomposition of zinc(II) dicarboxylates in a static air atmosphere. TGA, DTG and DSC curves for (a) $ZnC_3H_2O_4{\cdot}2H_2O$; (b) $Zn(C_4H_3O_4)_2{\cdot}2H_2O$; (c) $Zn(C_4H_5O_4)_2{\cdot}1.5H_2O$. Plot of $\log\sigma$ vs. T^{-1} for (d) $ZnC_3H_2O_4{\cdot}2H_2O$; (e) $Zn(C_4H_3O_4)_2{\cdot}2H_2O$; (f) $Zn(C_4H_5O_4)_2{\cdot}1.5H_2O$; (⊙) during decomposition; (×) cooling cycle.

Table 3
TGA–DTG–DSC data of zinc(II) dicarboxylates under static air atmosphere

Compound	TGA			DTG peak temperature (°C)	DSC peak temperature (°C)
	Mass loss (%)		Temperature range (°C)		
	Observed	Calculated			
Zinc(II) malonate dihydrate $ZnC_3H_2O_4{\cdot}2H_2O$	17.50	17.70	35–230	138.3	166.2 (endo.)
	50.67	51.38	230–380	360.7	388.6 (exo.)
Zinc(II) maleate dihydrate $Zn(C_4H_3O_4)_2{\cdot}2H_2O$	11.11	10.86	35–180	136.3	127.8 (endo.)
	39.99	39.27	180–250	185.2	160.7 (endo.)
	26.10	26.54	250–440	451.3	421.4 (exo.)
Zinc(II) succinate one and half hydrate $Zn(C_4H_5O_4)_2{\cdot}1.5H_2O$	7.77	8.27	35–130	110.0	100.3 (endo.)
	38.88	39.41	130–250	196.9	231.5 (endo.)
	27.77	28.33	250–500	498.2	485.0 (exo.)

observed. The elemental analyses agreed well with $ZnC_4H_2O_4$ (calculated, 39.27%; found, 39.99%) and $ZnC_4H_4O_4$ (calculated, 39.41%; found, 38.88%). Thus the partial decarboxylation of the maleate or succinate moiety was observed for these compounds.

The plot of log σ versus T^{-1} (Fig. 2(d) to (f)) showed a steady increase in the value of σ in the temperature range of 250 to 370°C (Region C). The parent samples heated isothermally in this region showed the infrared bands attributable to Zn–O stretching frequencies [35,36] became more intense and those due to coordinated carboxylate bands decrease in intensities. The X-ray diffraction pattern showed a generally sharp lines, and the pattern fits with the data for $ZnC_3H_2O_4$ (or $ZnC_4H_2O_4$ or $ZnC_4H_4O_4$) and ZnO. A steep increase in σ was observed at 380°C (Region D) between 380 and 440°C, Fig. 2(d) to (f). The infrared spectra and X-ray diffraction pattern for the parent samples decomposed isothermally at around 430°C showed mainly ZnO. The sample was white and had an electrical conductivity value of about $10^{-3}\,\Omega^{-1}\,cm^{-1}$ [37]. The sample thus obtained at 430°C shows a variation in σ with temperature. This behavior is characteristics of the non-stoichiometry present in ZnO [35–38].

Thus the conventional thermal analysis (TGA, DTG and DSC) supplemented with electrical conductivity, infrared spectra, X-ray diffraction patterns and elemental analyses gave a detailed analysis of the thermal decomposition of copper(II) and zinc(II) malonate, maleate and succinate complexes. It is well known that the solid-state thermal decomposition of metal dicarboxylates are influenced by the atmosphere [39–41]; it was decided to undertake similar measurements in other controlled atmospheres.

3.2.2. Dynamic dry nitrogen atmosphere

3.2.2.1. Copper(II) dicarboxylates. The dehydration of copper(II) malonate monohydrate ($CuC_3H_2O_4{\cdot}H_2O$), copper(II) maleate monohydrate ($CuC_4H_2O_4{\cdot}H_2O$) and copper(II) succinate half hydrate ($CuC_4H_4O_4{\cdot}0.5H_2O$) in Fig. 3(a) to (c) were clearly indicated by an endothermic peak in the DSC curves at around 160°C and a peak at same temperature in the DTG curves. The TGA curves showed a mass loss within the temperature range 50–225°C corresponding to the loss of water molecules. The decomposition of these complexes was indicated by an endothermic peak in the DSC curves at 300°C and in the DTG curves at the same temperature. The TGA curves showed a continuous mass loss from 225 to 420°C. These mass losses were found to be in good agreement with the formation of Cu_2O as the final product.

The temperature variation of the electrical conductivity σ (Fig. 3(d) to (f)) decreases steadily and remained constant upto 205°C (Region B) for copper(II) malonate and copper(II) succinate complexes, while a clear peak was shown at 140°C for copper(II) maleate complex. The infrared spectra, elemental analyses and X-ray diffraction pattern confirmed the formation of anhydrous copper(II) dicarboxylates in this region. After the dehydration step, the value of σ increased steadily within the temperature range

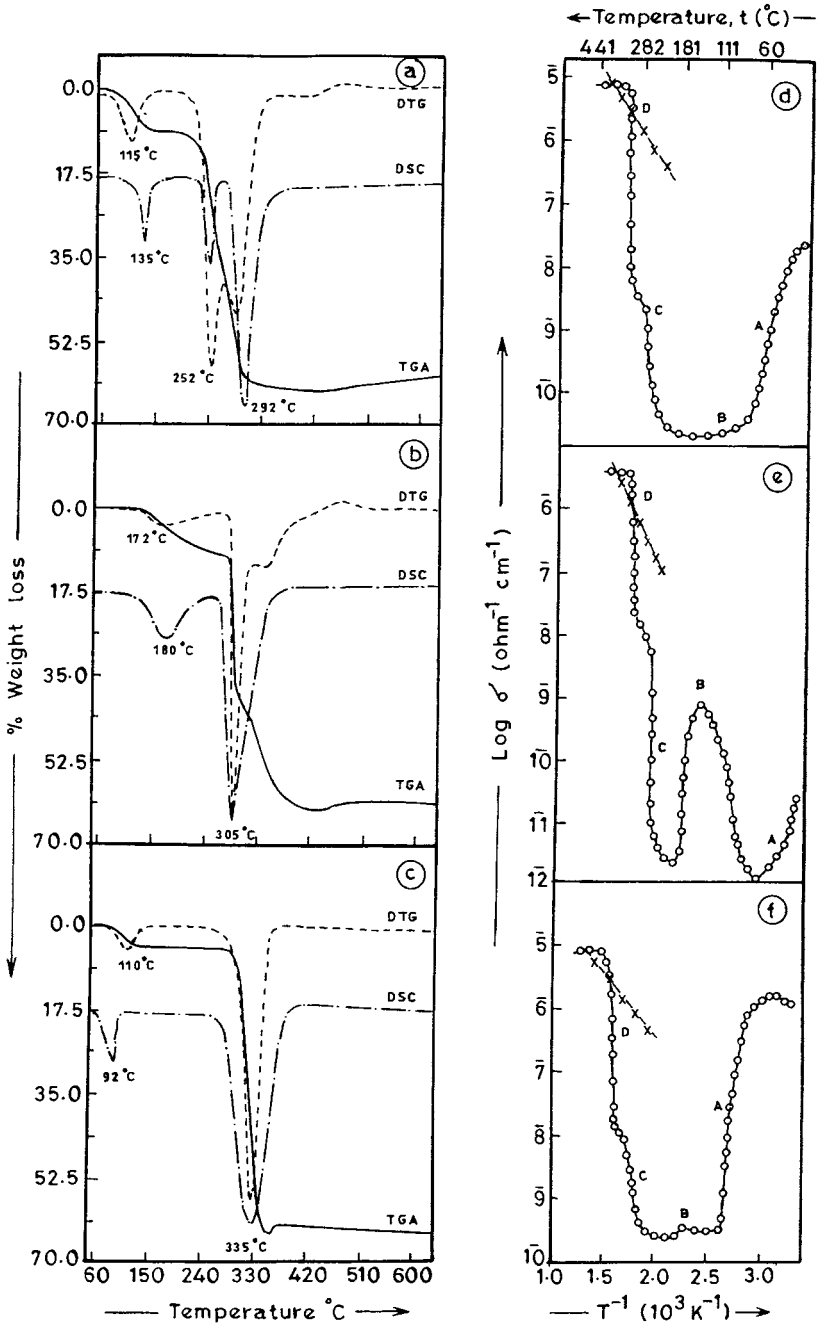

Fig. 3. Thermal decomposition of copper(II) dicaboxylates in a dynamic dry nitrogen atmosphere. TGA, DTG and DSC curves for (a) $CuC_3H_2O_4{\cdot}H_2O$; (b) $CuC_4H_2O_4{\cdot}H_2O$; (c) $CuC_4H_4O_4{\cdot}0.5H_2O$. Plot of $\log\sigma$ vs. T^{-1} for (d) $CuC_3H_2O_4{\cdot}H_2O$; (e) $CuC_4H_2O_4{\cdot}H_2O$; (f) $CuC_4H_4O_4{\cdot}0.5H_2O$; (⊙) during decomposition; (×) cooling cycle.

205–290°C (Region C) and then a steep increase in σ at 290–330°C (Region D). The X-ray diffraction patterns and infrared spectra for samples heated isothermally in Region C showed a mixture of anhydrous copper(II) dicarboxylates and Cu_2O.

The X-ray diffraction pattern for samples from the dry nitrogen atmosphere run obtained at 320°C (Region D) showed sharp lines and fitted well with the data for Cu_2O. The samples thus obtained at 320°C showed a variation in σ with changing temperature. This behavior is characteristics of Cu_2O [33]. The sample was red in color. Thus the X-ray diffraction patterns and conductivity measurements suggested that the products obtained by thermal decomposition of $CuC_3H_2O_4{\cdot}H_2O$, $CuC_4H_2O_4{\cdot}H_2O$ and $CuC_4H_4O_4{\cdot}0.5H_2O$ in a dry nitrogen atmosphere are pure Cu_2O, and that the concentration of copper metal, if present at all, are beyond the detection limits of these techniques.

3.2.2.2. Zinc(II) dicarboxylates. Thermal analysis (TGA, DTG and DSC) curves and the plot of log σ versus T^{-1} for $ZnC_3H_2O_4{\cdot}2H_2O$, $Zn(C_4H_3O_4)_2{\cdot}2H_2O$ and $Zn(C_4H_5O_4)_2{\cdot}1.5H_2O$ in nitrogen atmosphere were similar to the curves those obtained under static air atmosphere (see Fig. 2(a) to (f)).

The isothermal decomposition study under this atmosphere demonstrated that the intermediates and final product were similar to static air atmosphere.

Thermal stabilities of dehydration and decompositions for copper(II) and zinc(II) malonate, maleate and succinate complexes are slightly higher in nitrogen than static air atmosphere. The stability sequences of these complexes are similar in both the atmospheres.

The prescribed intermediates are obtained in each temperature region of dc electrical conductivity measurements under static air and dynamic dry nitrogen atmosphere are shown in Tables 4 and 5. The gaseous products obtained by the thermal decomposition of copper(II) dicarboxylates or zinc(II) dicarboxylates under dynamic (pure and dry) nitrogen atmosphere were analyzed by qualitative gas detection method as described in [25].

These gases were also confirmed by gas liquid chromatography (not shown). These chromatograms showed the presence of both polar and non-polar gases. The gases were collected at ca. 380°C.

The different paths followed by the decomposition of copper(II) and zinc(II) malonate, maleate and succinate in different atmospheres showed complete dehydration, as was seen from conductivity measurements and the infrared spectra. A transformation of anhydrous copper(II) dicarboxylates to Cu_2O was also detected in static air atmosphere. A separate phase of Cu_2O could not be obtained; this compound always occurred with anhydrous copper(II) dicarboxylates. Thus, the transformation of Cu_2O and anhydrous copper(II) dicarboxylates seems to be an equilibrium reaction. This mixture of Cu_2O and anhydrous copper(II) dicarboxylates is then transformed to CuO which is the final product obtained in static air atmosphere. These reactions are presented as follows.

Copper(II) malonate monohydrate

$$CuC_3H_2O_4 \cdot H_2O \overset{35-170^{\circ}C}{\rightarrow} CuC_3H_2O_4 + H_2O\,(g) \quad (1)$$

$$3CuC_3H_2O_4 \overset{170-275^{\circ}C}{\rightarrow} CuC_3H_2O_4 + Cu_2O + C_2H_4\,(g) + CO\,(g) + 3CO_2\,(g) \quad (2)$$

$$CuC_3H_2O_4 + Cu_2O \overset{275-380^{\circ}C}{\rightarrow} 3CuO + C_2H_2\,(g) + CO_2\,(g) \quad (3)$$

Copper(II) maleate monohydrate

$$CuC_4H_2O_4 \cdot H_2O \overset{35-210^{\circ}C}{\rightarrow} CuC_4H_2O_4 + H_2O\,(g) \quad (4)$$

$$3CuC_4H_2O_4 \overset{210-280^{\circ}C}{\rightarrow} CuC_4H_2O_4 + Cu_2O + C_2H_4\,(g) + 5CO\,(g) + CO_2\,(g) \quad (5)$$

$$CuC_4H_2O_4 + Cu_2O \overset{280-375^{\circ}C}{\rightarrow} 3CuO + C_2H_2\,(g) + 2CO\,(g) \quad (6)$$

Copper(II) succinate half hydrate

$$CuC_4H_4O_4 \cdot 0.5H_2O \overset{35-180^{\circ}C}{\rightarrow} CuC_4H_4O_4 + 0.5H_2O\,(g) \quad (7)$$

$$3CuC_4H_4O_4 \overset{180-280^{\circ}C}{\rightarrow} CuC_4H_4O_4 + Cu_2O + 2C_2H_4\,(g) + CO\,(g) + 3CO_2\,(g)$$

$$0.5CuC_4H_4O_4 + Cu_2O \overset{280-385^{\circ}C}{\rightarrow} 2.5CuO + 0.5C_2H_2\,(g) + 0.25C_2H_4\,(g) + 0.5CO\,(g) \quad (9)$$

The transformation of anhydrous copper(II) dicarboxylates to Cu_2O was the final step detected in a dynamic dry nitrogen atmosphere, while $ZnC_3H_2O_4$,$Zn(C_4H_3O_4)_2$ and $Zn(C_4H_5O_4)_2$ transformed to ZnO under static air as well dynamic dry nitrogen

Table 4
Predicted products formed at each decomposition stage of copper(II) dicarboxylates under static air and dynamic dry nitrogen atmospheres by dc electrical conductivity measurements

Compound	Static air			Dry nitrogen		
	Region	Temperature range (°C)	Predicted intermediates and final products	Region	Temperature range (°C)	Predicted intermediates and final products
Copper(II) malonate monohydrate $CuC_3H_2O_4{\cdot}H_2O$	A	35–85	$CuC_3H_2O_4{\cdot}H_2O$	A	35–90	$CuC_3H_2O_4{\cdot}H_2O$
	B	85–170	$CuC_3H_2O_4$	B	90–200	$CuC_3H_2O_4$
	C	170–275	$CuC_3H_2O_4 + Cu_2O$	C	200–280	$CuC_3H_2O_4 + Cu_2O$
	D	275–310	$CuC_3H_2O_4 + Cu_2O + CuO$	D	280–330	Cu_2O
	E	310–380	CuO			
Copper(II) maleate monohydrate $CuC_4H_2O_4{\cdot}H_2O$	A	35–90	$CuC_3H_2O_4{\cdot}H_2O$	A	35–95	$CuC_3H_2O_4{\cdot}H_2O$
	B	90–210	$CuC_3H_2O_4$	B	95–195	$CuC_3H_2O_4$
	C	210–280	$CuC_3H_2O_4 + Cu_2O$	C	195–285	$CuC_3H_2O_4 + Cu_2O$
	D	280–305	$CuC_3H_2O_4 + Cu_2O + CuO$	D	285–350	Cu_2O
	E	305–375	CuO			
Copper(II) succinate half hydrate $CuC_4H_4O_4{\cdot}0.5H_2O$	A	35–85	$CuC_4H_4O_4{\cdot}0.5H_2O$	A	35–90	$CuC_4H_4O_4{\cdot}0.5H_2O$
	B	85–180	$CuC_4H_4O_4$	B	90–205	$CuC_4H_4O_4$
	C	180–280	$CuC_4H_4O_4 + Cu_2O$	C	205–300	$CuC_4H_4O_4 + Cu_2O$
	D	280–315	$CuC_4H_4O_4 + Cu_2O + CuO$	D	300–360	Cu_2O
	E	315–385	CuO			

Table 5
Predicted products formed at each decomposition stage of zinc(II) dicarboxylates under static air and dynamic dry nitrogen atmospheres by dc electrical conductivity measurements

Compound	Static air			Dry nitrogen		
	Region	Temperature range (°C)	Predicted intermediates and final products	Region	Temperature range (°C)	Predicted intermediates and final products
Zinc(II) malonate dihydrate	A	35–90	$ZnC_3H_2O_4{\cdot}2H_2O$	A	40–90	$ZnC_3H_2O_4{\cdot}2H_2O$
$ZnC_3H_2O_4{\cdot}2H_2O$	B	90–230	$ZnC_3H_2O_4$	B	90–235	$ZnC_3H_2O_4$
	C	230–300	$ZnC_3H_2O_4 + ZnO$	C	235–305	$ZnC_3H_2O_4 + ZnO$
	D	300–380	ZnO	D	305–385	ZnO
Zinc(II) maleate dihydrate	A	35–95	$Zn(C_4H_3O_4)_2{\cdot}2H_2O$	A	35–95	$Zn(C_4H_3O_4)_2{\cdot}2H_2O$
$Zn(C_4H_3O_4)_2{\cdot}2H_2O$	B	95–180	$Zn(C_4H_3O_4)_2$	B	95–185	$Zn(C_4H_3O_4)_2$
	B′	180–250	$ZnC_4H_2O_4$	B′	185–255	$ZnC_4H_2O_4$
	C	250–390	$ZnC_4H_2O_4 + ZnO$	C	255–390	$ZnC_4H_2O_4 + ZnO$
	D	390–440	ZnO	D	390–445	ZnO
Zinc(II) succinate one and half hydrate	A	35–90	$Zn(C_4H_5O_4)_2{\cdot}1.5H_2O$	A	40–95	$Zn(C_4H_5O_4)_2{\cdot}1.5H_2O$
$Zn(C_4H_5O_4)_2{\cdot}1.5H_2O$	B	90–130	$Zn(C_4H_5O_4)_2$	B	95–135	$Zn(C_4H_5O_4)_2$
	B′	130–250	$ZnC_4H_4O_4$	B′	135–255	$ZnC_4H_4O_4$
	C	250–385	$ZnC_4H_4O_4 + ZnO$	C	255–390	$ZnC_4H_4O_4 + ZnO$
	D	385–445	ZnO	D	390–450	ZnO

atmospheres. The proposed scheme for thermal decomposition of these complexes is as follows.

Zinc(II) malonate dihydrate

$$ZnC_3H_2O_4 \cdot 2H_2O \overset{35-230^{\circ}C}{\rightarrow} ZnC_3H_2O_4 + 2H_2O\,(g) \quad (10)$$

$$2ZnC_3H_2O_4 \overset{230-300^{\circ}C}{\rightarrow} ZnC_3H_2O_4 + ZnO + 0.5C_2H_4\,(g) + CO\,(g) + CO_2\,(g) \quad (11)$$

$$0.2ZnC_3H_2O_4 + 0.8ZnO \overset{300-380^{\circ}C}{\rightarrow} ZnO + 0.1C_2H_4\,(g) + 0.2CO\,(g) + 0.2CO_2\,(g) \quad (12)$$

Zinc(II) maleate dihydrate

$$Zn(C_4H_3O_4)_2 \cdot 2H_2O \overset{35-180^{\circ}C}{\rightarrow} Zn(C_4H_3O_4)_2 + 2H_2O\,(g) \quad (13)$$

$$Zn(C_4H_3O_4)_2 \overset{180-250^{\circ}C}{\rightarrow} ZnC_4H_2O_4 + C_2H_4\,(g) + 2CO_2\,(g) \quad (14)$$

$$ZnC_4H_2O_4 \overset{250-390^{\circ}C}{\rightarrow} 0.3ZnC_4H_2O_4 + 0.7ZnO + 0.3C_2H_2\,(g) + 0.2C_2H_4\,(g) + 1.5CO\,(g) + 0.3CO_2\,(g) \quad (15)$$

$$0.3ZnC_4H_2O_4 + 0.7ZnO \overset{390-440^{\circ}C}{\rightarrow} ZnO + 0.1C_2H_2\,(g) + 0.1C_2H_4\,(g) + 0.7CO\,(g) + 0.1CO_2\,(g) \quad (16)$$

Zinc(II) succinate one and half hydrate

$$Zn(C_4H_5O_4)_2 \cdot 1.5H_2O \overset{35-130^{\circ}C}{\rightarrow} Zn(C_4H_4O_4)_2 + 1.5H_2O\,(g) \quad (17)$$

$$Zn(C_4H_5O_4)_2 \overset{130-250^{\circ}C}{\rightarrow} ZnC_4H_4O_4 + C_2H_4\,(g) + H_2O\,(g) + CO\,(g) + CO_2\,(g) \quad (18)$$

$$ZnC_4H_4O_4 \overset{250-385^{\circ}C}{\rightarrow} 0.3ZnC_4H_4O_4 + 0.7ZnO + 0.7C_2H_4\,(g) + 0.7CO\,(g) + 0.7CO_2\,(g) \quad (19)$$

$$0.3ZnC_4H_4O_4 + 0.7ZnO \overset{385-445^{\circ}C}{\rightarrow} ZnO + 0.3C_2H_4\,(g) + 0.3CO\,(g) + 0.3CO_2\,(g) \quad (20)$$

4. Conclusions

The present study suggested the following important points in the solid-state decomposition of copper(II) and zinc(II) dicarboxylates.

In dry nitrogen, the formation of Cu_2O from $CuC_3H_2O_4 \cdot H_2O$, $CuC_4H_2O_4 \cdot H_2O$ and $CuC_4H_4O_4 \cdot 0.5H_2O$ were confirmed by using dc electrical conductivity measurements, in conjunction with infrared spectra and X-ray diffraction investigations.

The final product of decomposition in static air was found to be CuO for copper(II) malonate, copper(II) maleate and copper(II) succinate complexes. However, the final decomposition product in both the atmosphere were found to be ZnO for zinc(II) malonate, zinc(II) maleate and zinc(II) succinate complexes.

The oxidative behavior of these complexes was better understood from the study of temperature variation of dc electrical conductivity measurements.

Acknowledgements

This work was supported by U.G.C., New Delhi. The teacher fellowship scheme (SKP) was awarded.

References

[1] W.E. Brown, D. Dollimore, A.K. Galway, Comprehensive Chemical Kinetics, Vol. 22, Elsevier, Amsterdam, 1980.
[2] D. Dollimore, T.A. Evans, Y.F. Lee, Thermochim. Acta 194 (1992) 215.
[3] D. Dollimore, D.L. Griffiths, J. Therm. Anal. 2 (1970) 229.
[4] V.V. Bolydrev, I.S. Nev'Yantsev, Y.I. Mikhailov, E.F. Khairetdinov, Kinet. Katal. 11 (1970) 367.
[5] N.J. Carr, A.K. Galway, Proc. R. Soc. London Ser. A 404 (1986) 101.
[6] N.J. Carr, A.K. Galway, J. Chem. Soc., Faraday Trans. 1.84 (1988) 1357.
[7] M.J. McGinn, B.R. Wheeler, A.K. Galway, Trans. Faraday. Soc. 67 (1971) 1.
[8] J.R. Allan, G.M. Baillie, J.G. Bonner, D.L. Gerrard, S. Hoey, Thermochim. Acta 143 (1989) 283.
[9] K.M.A. El-Salaam, K.H. Halawani, S.A. Fakiha, Thermochim. Acta 204 (1992) 331.
[10] W. Brzyska, B. Galkowska, Polish J. Chem. 72 (1998) 498.
[11] J.R. Allan, B.R. Carson, D.L. Gerrard, S. Hoey, Thermochim. Acta 158 (1990) 91.
[12] H. Yokobayashi, K. Nagase, K. Muraishi, Bull. Chem. Soc. Jpn. 48 (10) (1975) 2789.
[13] Le V. My, G. Perinet, R. Lafont, C. R. Acad. Sci. Paris Ser. C 268 (1969) 406.
[14] V.P. Sevost'yanov, L.M. Dvornikova, Zh. Neorg. Khim. 16 (1971) 1812.
[15] K. Nagase, K. Muraishi, K. Sone, N. Tanaka, Bull. Chem. Soc. Jpn. 48 (1975) 3184.

[16] W.E. Brown, D. Dollimore, A.K. Galway, in: C.H. Banford, C.F.H. Tipper (Eds.), Comprehensive Chemical Kinetics, Vol. 22, Reaction in the Solid State, Elsevier, Amsterdam, 1980, p. 208.
[17] K.A. Jones, R.J. Acheson, B.R. Wheeler, A.K. Galway, Trans. Faraday Soc. 64 (7) (1968) 1887.
[18] K. Muraishi, K. Nagase, N. Tanaka, Thermochim. Acta 23 (1978) 125.
[19] A.K. Galway, S.G. Mckee, T.R.B. Mitchell, M.A. Mohamed, M.E. Brown, A.F. Bean, React. Solids 6 (2/3) (1988) 187.
[20] J.R. Allan, B.R. Carson, D.L. Gerrard, S. Hoey, Thermochim. Acta 147 (1989) 353.
[21] R.L. Schmid, J. Felsche, Thermochim. Acta 59 (1982) 105.
[22] V. Frei, J. Ederova, Collect. Czech. Chem. Commun. 34 (1969) 1304.
[23] S. Ghosh, S.K. Ray, P.K. Ray, T.K. Banerjee, J. Indian Chem. Soc. LXI (1984) 850.
[24] J.R. Allan, J.G. Bonner, H.J. Bowley, D.L. Gerrard, S. Hoey, Thermochim. Acta 141 (1989) 227.
[25] A.K. Nikumbh, S.K. Pardeshi, S.B. Mane, J. Therm. Anal. (2001), sent for publication.
[26] K.S. Rane, A.K. Nikumbh, A.J. Mukhedkar, J. Mater. Sci. 16 (1981) 2387.
[27] A.K. Nikumbh, A.E. Athare, V.B. Raut, Thermochim. Acta 186 (1989) 217.
[28] G.B. Deacon, R.J. Philips, Coord. Chem. Rep. 33 (1980) 227.
[29] A.C. Ranade, V.V. Subba Rao, Indian J. Chem. 4 (1966) 42.
[30] P.S. Bassi, B.S. Randhawa, C.M. Khajuria, S. Kaur, J. Therm. Anal. 32 (1987) 569.
[31] K. Nagase, Bull. Chem. Soc. Jpn. 45 (1972) 2166.
[32] J. Fujita, A. E. Martell, K. Nakamoto, J. Chem. Phys. 36 (1962) 324, 331.
[33] A.P. Young, C.M. Schwartz, J. Phys. Chem. Solids 30 (1969) 249.
[34] F.A. Cotton, G. Wilkinson, Advanced Inorganic Chemistry, Interscience Publications, New York, 1972, p. 114.
[35] R.A. Nyquist, R.O. Kagel, in Infrared Spectra of Inorganic Molecules, Academic Press, London, 1971, p. 221.
[36] D.K. Jain, J.C. Garg, Indian J. Pure Appl. Phys. 17 (1979) 10.
[37] A.V. Krylova, L. Ya Margolis, G.I. Chizhikova, Kinetika Katali 6 (5) (1965) 771.
[38] W.J. Moore, Seven Solid States: An Introduction to Chemistry and Physics of Solids, W.A. Benjamin, Inc., New York, 1967, p. 145.
[39] E.D. Macklen, J. Inorg. Nucl. Chem. 30 (1968) 2689.
[40] D. Dollimore, D.L. Griffiths, D. Nicholson, J. Chem. Soc. (1963) 2617.
[41] Y. Suzuki, K. Muraishi, Hiroko Ito, Thermochim. Acta 258 (1995) 231.